TIGERISS Expected Observation Prediction Model Updates

William Labrador, Brian Rauch, Wolfgang Zober, Scott Nutter

Galactic Cosmic Rays

- Galactic cosmic rays (GCRs) are charged particles originating in the Milky Way.
- Of all GCR nuclei, ~89% is hydrogen and ~10% is helium, with the remaining 1% being heavier elements.
- Stellar fusion from stars like the Sun can create elements up to $_{26}$Fe.
- Supernova shocks accelerate cosmic rays above the MeV range.

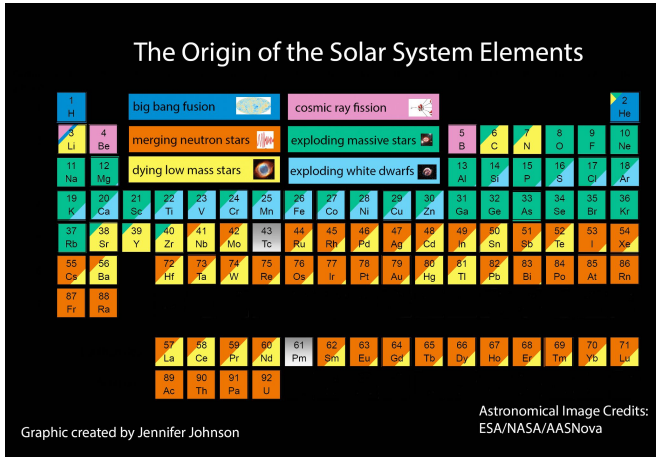

Ultra-heavy Galactic Cosmic Ray Creation and Acceleration

- OB Associations are a major source of r-process nucleosynthesis events which are responsible for the creation of about half of all ultra-heavy galactic cosmic rays (UHGCRs).
- Elements are classified by condensation temperature into refractories (T_c>1250K) and volatiles (T_c<1250K). Refractory elements condense onto dust grains, which are preferentially accelerated by supernova shocks due to their higher rigidity.

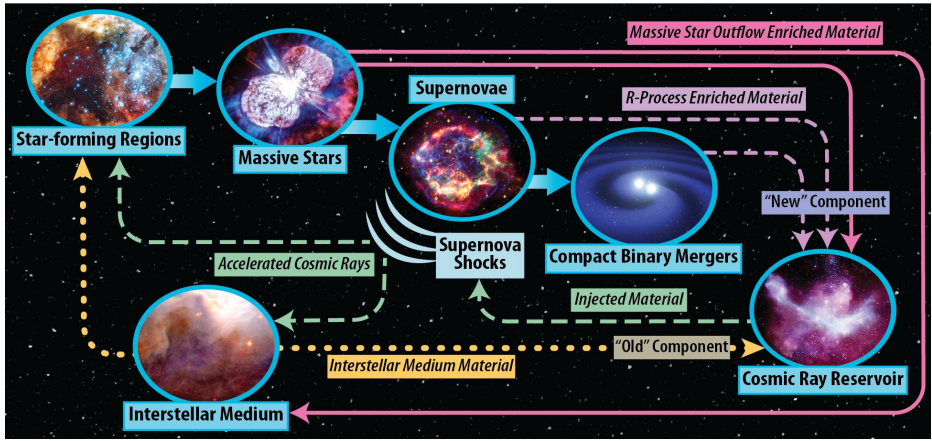

SuperTIGER Results

- In 2012-2013, SuperTIGER flew for a record-setting 55 days, allowing measurements for single element UHGCR measurements up to Z=56.
- Past Z=40, SuperTIGER observed a break in the OB association model supported by previous cosmic ray experiments, suggesting a new source of r-process nucleosynthesis.

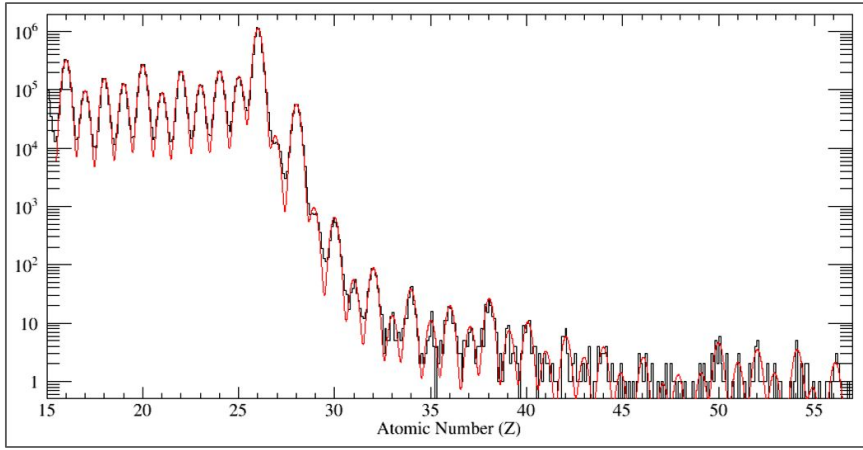

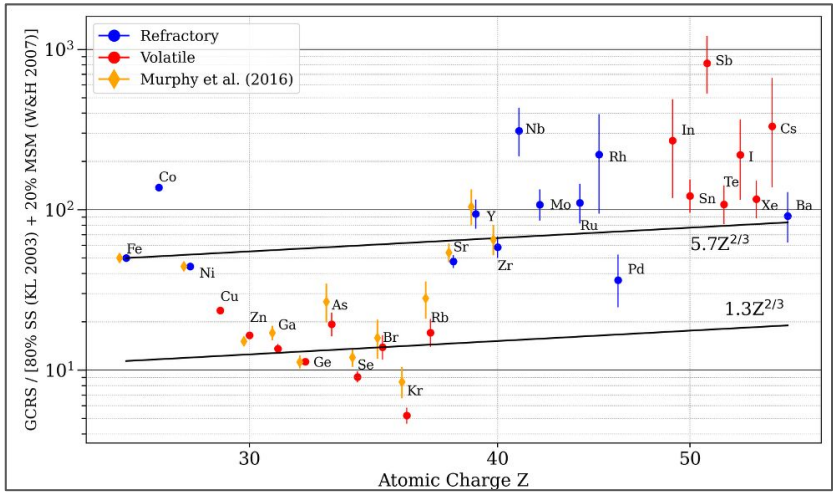

TIGERISS

- TIGERISS will make the first single-element measurements of UHGCRs up to Z=82.
- Within 1 year of flight, TIGERISS will match SuperTIGER's first flight statistics.

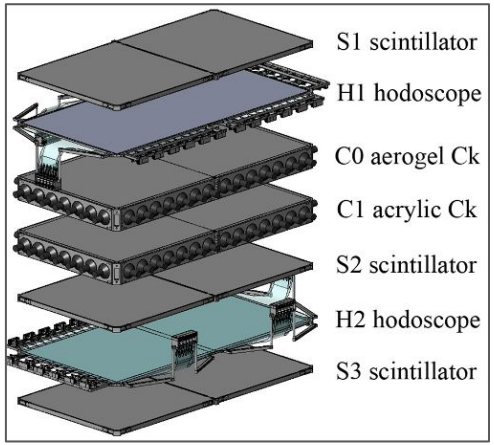

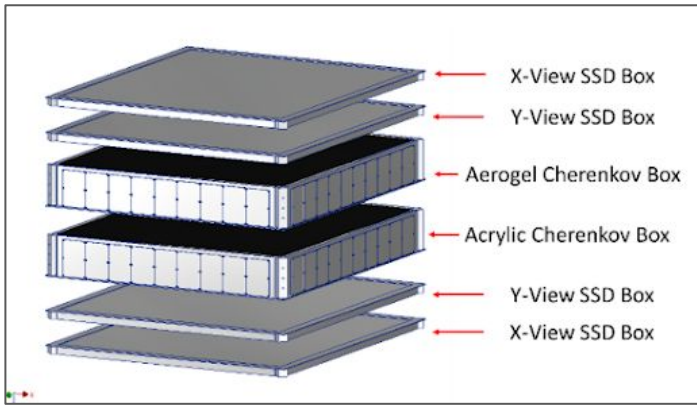

From SuperTIGER to TIGERISS

SuperTIGER: Balloon-borne Experiment

- Flies within the atmosphere, requiring atmospheric corrections

TIGERISS: Space-based Experiment

- Trades a smaller detector area for a longer measurement period
- Will fly within the magnetic field, requiring rigidity cutoff corrections

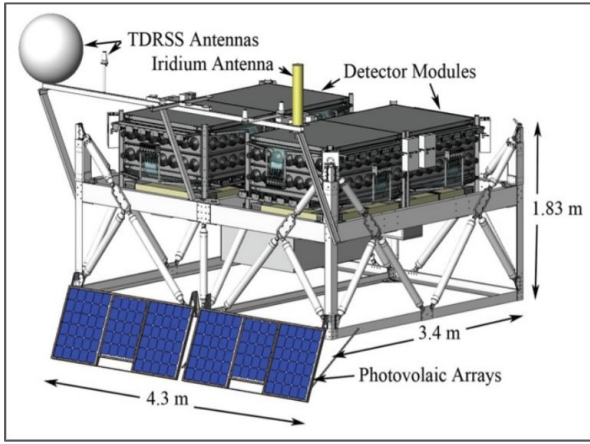

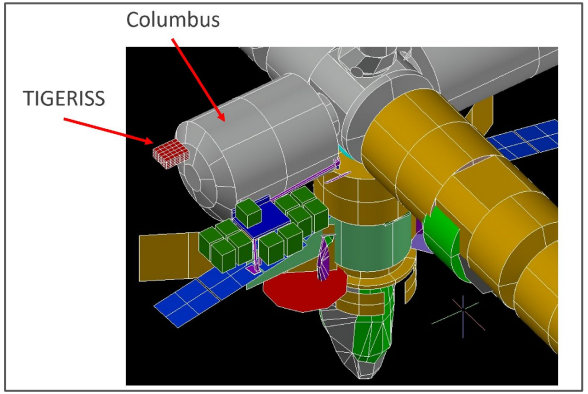

TIGERISS Prediction Model

- Integrated energy spectra are derived using ACE-CRIS measurements for solar maximum and minimum, and HEAO-3-C2 at higher energies.
- We use 2D differential geometry factors as a function of East-West inclination angle to account for geomagnetic screening effects.
- Geomagnetic rigidity cutoffs and top-of-instrument energy thresholds are both used to evaluate events.

Updating Material Interactions

- Early TIGERISS predictions used SuperTIGER materials as an initial attempt at making survival fraction calculations.
- TIGERISS will require different material densities and chemical compositions in the transition to spaceflight.

Original Materials	Updated Materials
Acrylic (1.4986 g/cm^2)	Acrylic (1.5113 g/cm^2)
Aerogel (0.41 g/cm^2)	Aerogel (0.400304 g/cm^2)
Silicon (0.9316 g/cm^2)	Silicon (0.473253 g/cm^2)
Aluminum (0.4536 g/cm^2)	Aluminum (0.6858 g/cm^2)
Kapton (0.01803 g/cm^2)	Kapton (0.173126 g/cm^2)
PMI (0.2794 g/cm^2)	Epoxy (0.394818 g/cm^2)
PET(0.102 g/cm^2)	Rohacell (0.243352 g/cm^2)
PS (0.083 g/cm^2)	MLI (2.6% Al, 24.5% Kapton, 33.6% polyester, 39.3% mylar) (0.059592 g/cm^2)
PTFE (0.06 g/cm^2)	Goretex (0.031369 g/cm^2)
PU (0.0508 g/cm^2)	Beta Cloth (98% glass, 2% teflon) (0.026119 g/cm^2)
PE (0.00552 g/cm^2)	Polyester (0.014224 g/cm^2)
	DFab (55% kevlar, 45% kapton) (0.011557 g/cm^2)

Updating Material Interactions

Events where spallation occurs will be discarded during charge-consistency cuts. A top-of-instrument (TOI) correction is made to account for charge-changing interactions within the detector using Nilsen cross sections.

$$N_{\mathrm{TOI}}(Z) = N_{\mathrm{INS}}(Z) \prod_i \exp\left[\frac{x_i}{\lambda_i(Z)} (\sec\theta_{\mathrm{Fe}})\right]$$

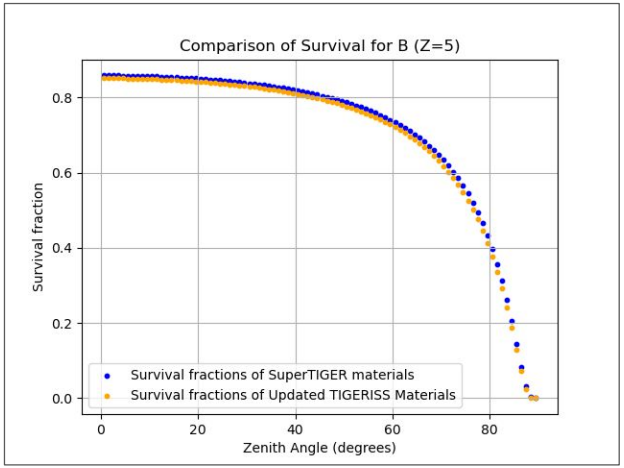

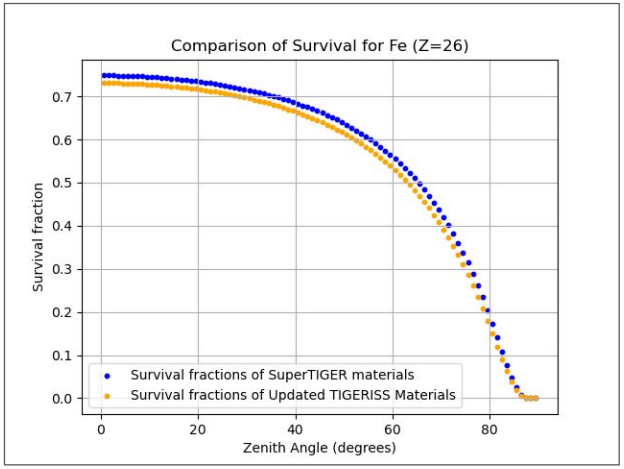

Geomagnetic Orientation

- Previous predictions averaged two orientations of the major and minor axes being aligned with geomagnetic north.
- TIGERISS will fly aboard the ISS, traveling between ±51.6º. As the ISS changes latitude, TIGERISS will experience orientation changes.

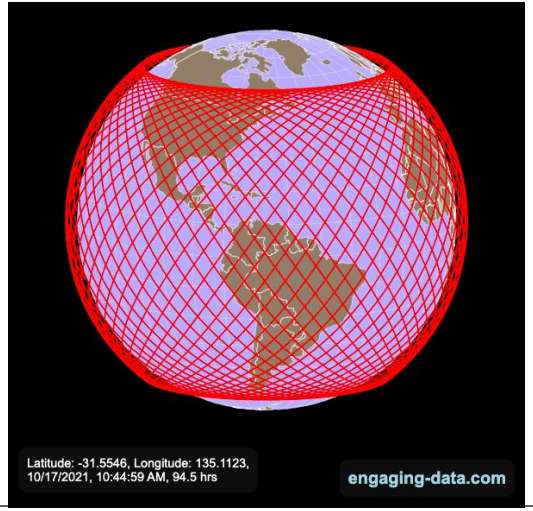

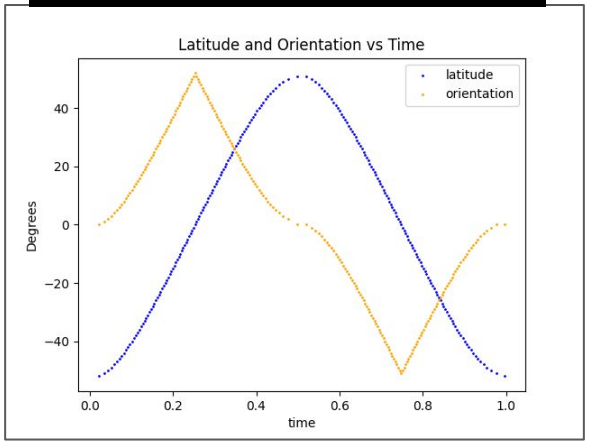

Geomagnetic Orientation

ISS orientation and magnetic field declination are combined to determine a geomagnetic orientation. Geometry factors for each geomagnetic orientation are calculated and used in the prediction model, using weighting based on the percentage of time spent at each latitude.

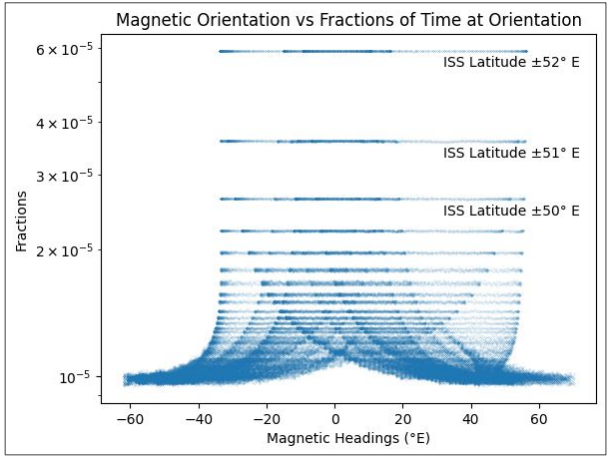

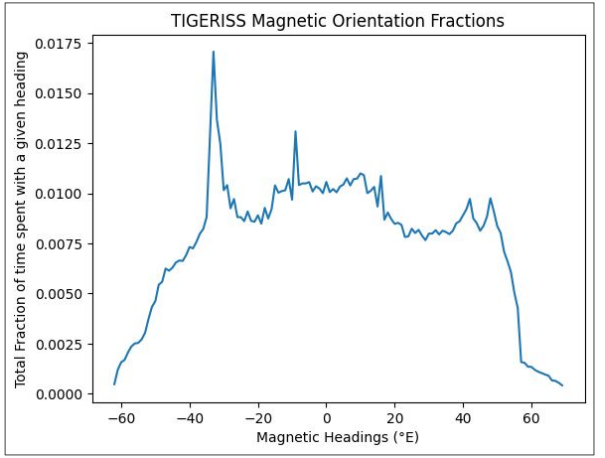

ISS Obstructions

TIGERISS will lose events to obstructions from the ISS structure. Using Geant4 simulations, geometries of the obstructions are used to remove events from the total count.

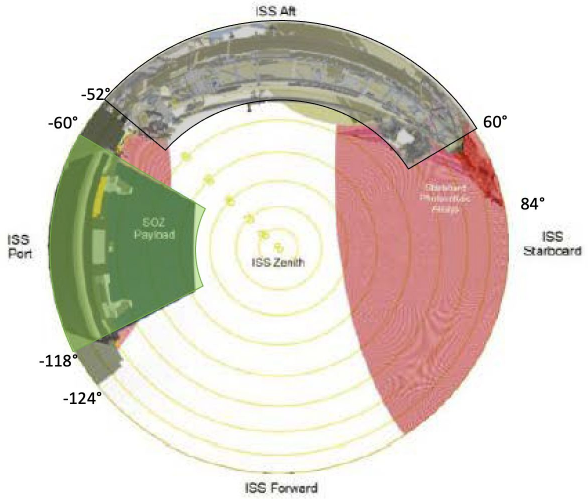

Removed geometry in shaded shapes.

NB: Azimuth angles of Slides 5-6 rotated by 180° to convert from upward (particle incidence) to downward (instrument zenith).

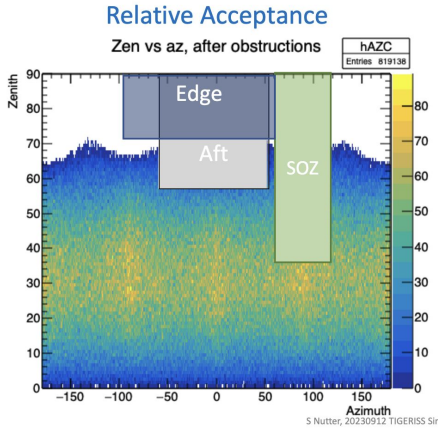

TIGERISS Current Predictions

We have updated our TIGERISS predictions to account for the mature instrument materials, orientation within the geomagnetic field, and obstructions from the ISS.

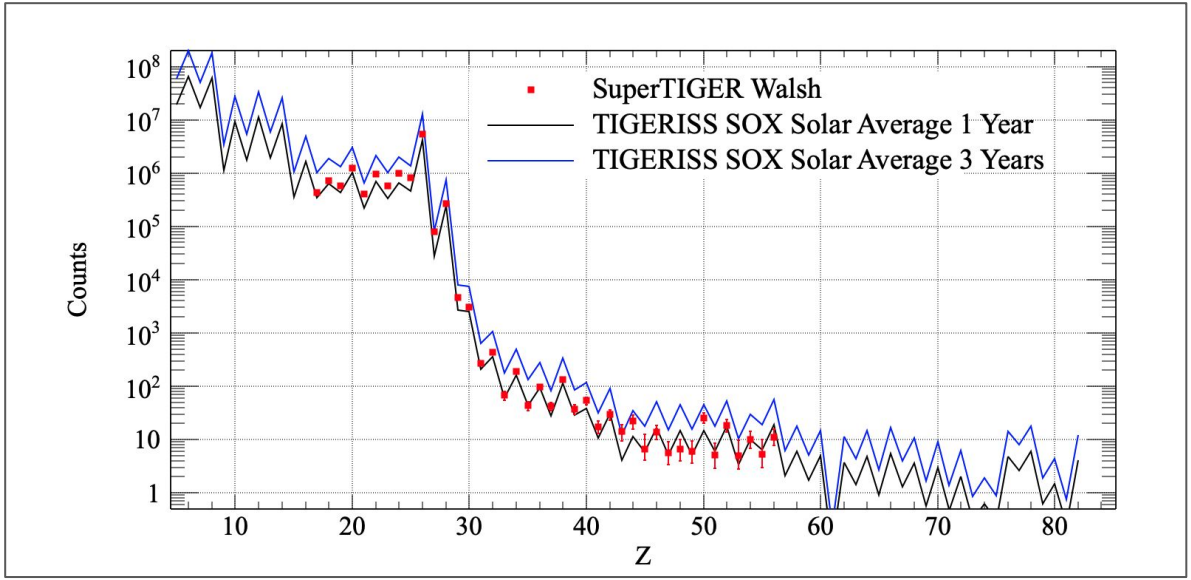

Future Work

HELMOD spectra are being incorporated into the predictions model to reflect the solar cycle.

Future updates will consider the effects of space weather on the geomagnetic field and rigidity cutoffs.

References

1) B. F. Rauch, W. V. Zober, Q. Abarr, Y. Akaike, W. R. Binns, R. F. Borda, R. G. Bose, T. J. Brandt, D. L. Braun, J. H. Buckley, et al., Instruments 8 (2024), ISSN 2410-390X, URL https://www.mdpi.com/2410-390X/8/1/4.
2) Rauch, Brian F. et al. “Modeling Expected TIGERISS Observations.” Proceedings of 38th International Cosmic Ray Conference — PoS(ICRC2023) (2023): n. Pag.
3) B. Rauch, Advances in Space Research 53, 1444 (2014), ISSN 0273-1177, cosmic Ray Origins: Viktor Hess Centennial Anniversary, URL https://www.sciencedirect.com/science/article/pii/S027311771300642X.
4) D.F. Smart, M.A. Shea, A review of geomagnetic cutoff rigidities for earth-orbiting spacecraft, Advances in Space Research, Volume 36, Issue 10, 2005, Pages 2012-2020, ISSN 0273-1177.
5) B. S. Nilsen, C. J. Waddington, J. R. Cummings, T. L. Garrard, and J. Klarmann, Physical Review C 52, 3277 (1995).

TIGERISS Collaboration

B. Abresch[1], H. Allen[2], R. F. Borda[3], R. G. Bose[4], J. Calderon[5], N. W. Cannady[6], J.L. Champion[7], M. Clark[8], J. Coldsmith[7], N. Cordrey[1], S. Coutu[2], T. Forstmeier[2], M. Fratta[1], C. Fredlund[7], P. Ghosh[3,6,9], S. Gordon[7], S. Graham[7], T. Green[1], D. W. Harmon[7], H. Jeon[7], C. Jones[7], S. Jones[5], J. F. Krizmanic[6], W. Labrador[4], J. V. Martins[3], M. P. McPherson[8], J. W. Mitchell[6], S. I. Mognet[2], T. L. Ng[1], G. A. de Nolfo[10], S. Nutter[5], N. Osborn[4], M. Pant[5], I. M. Pastrana[4], D. Radomski[4], B. F. Rauch[4], K. Sakai[11], M. Sasaki[12,6,9,] S. Singh[7], S. Smith[8], L. Tian[7], H. A. Tolentino[8], Y. Tufail[1], S. Wall[7], D. Washington[2], T. Widmeyer[7], L. Williams[7], W. V. Zober[4],

[1]NASA Wallops Flight Center, [2] Pennsylvania State University, [3]University of Maryland, Baltimore County, [4]Department of Physics and McDonnell Center for the Space Sciences, Washington University in St. Louis, [5]Northern Kentucky University, [6]NASA Goddard Space Flight Center, Astrophysics Science Division, [7]NASA Goddard Space Flight Center, [8]Howard University, [9]Center for Research and Exploration in Space Sciences and Technology II, [10]University of Chicago, [11]University of Maryland, College Park

Acknowledgments

This work was supported by NASA Astrophysics Pioneers Program cooperative agreement 80NSSC22M0299. TIGERISS has been supported at Washington University in St. Louis by a grant from the Peggy and Steve Fossett Foundation and by the McDonnell Center for the Space Sciences. TIGERISS builds on work under NASA grants for CALET(NNX11AE02G, NNX16AC02G, and 80NSSC20K0399) and SuperTIGER (NNX15AC23G and 80NSSC20K0405). We thank the NASA Columbia Scientific Balloon Facility, the NASA Balloon Program Office, and the NSF United States Antarctic Program for the 55-day long-duration balloon flight for SuperTIGER-1, the 32-day SuperTIGER-2.3 flight, and the successful recovery efforts, which provided scientific and technical background for TIGERISS.

The material contained in this document is based upon work supported by a National Aeronautics and Space Administration (NASA) grant or cooperative agreement. Any opinions, findings,conclusions, or recommendations expressed in this material are those of the author and do not necessarily reflect the views of NASA.

Extra Slides

Geomagnetic Orientation

Using the World Magnetic Model, we find magnetic field declinations, the angular difference between geographic and magnetic north for every location of the ISS.

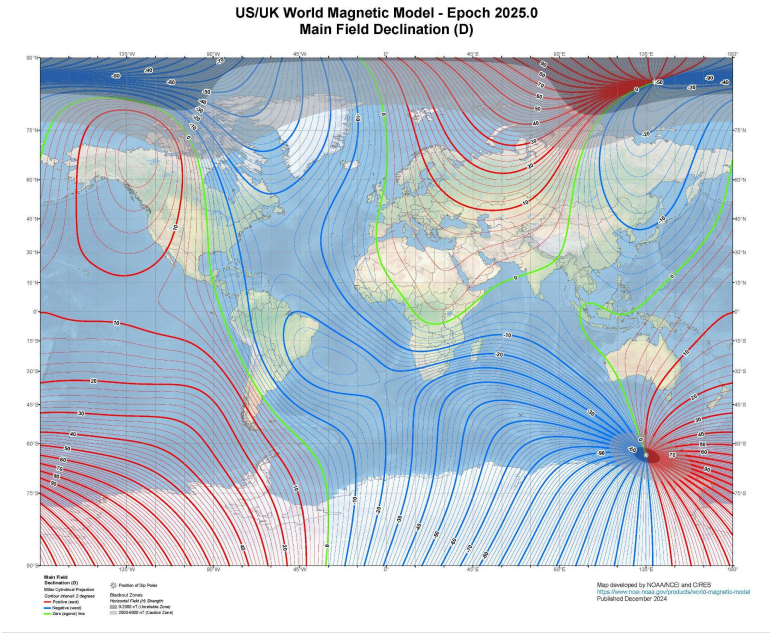

Stoermer Approximation

$$R_c = [M\cos^4\lambda]/\{r^2[1+(1-\sin\epsilon\sin\xi\cos^3\lambda)^{1/2}]^2\}$$

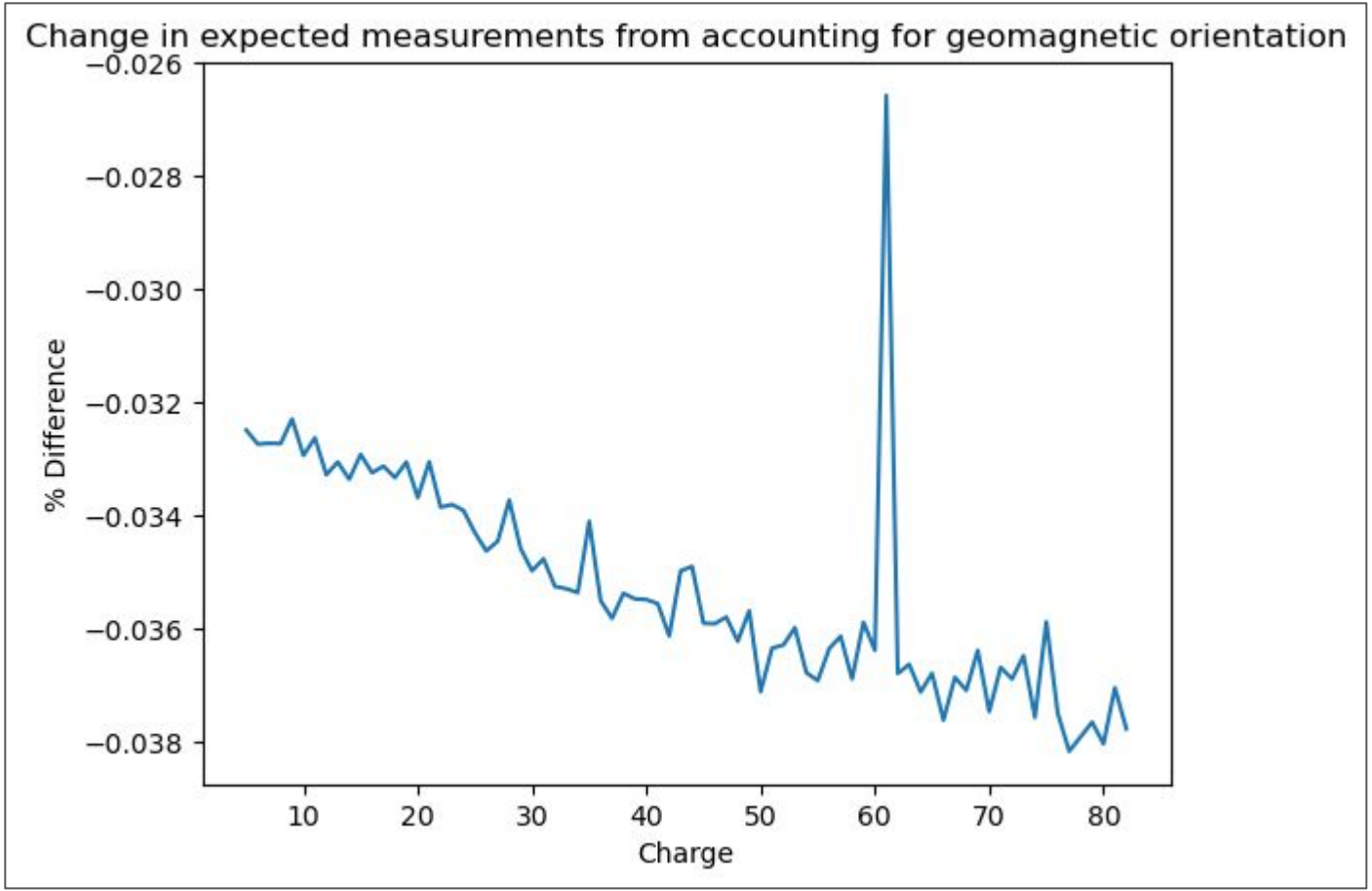
Change in expected measurements from accounting for geomagnetic orientation
−0.026
−0.028
−0.030
−0.032
−0.034
−0.036
−0.038
% Difference
10
20
30
40
50
60
70
80
Charge

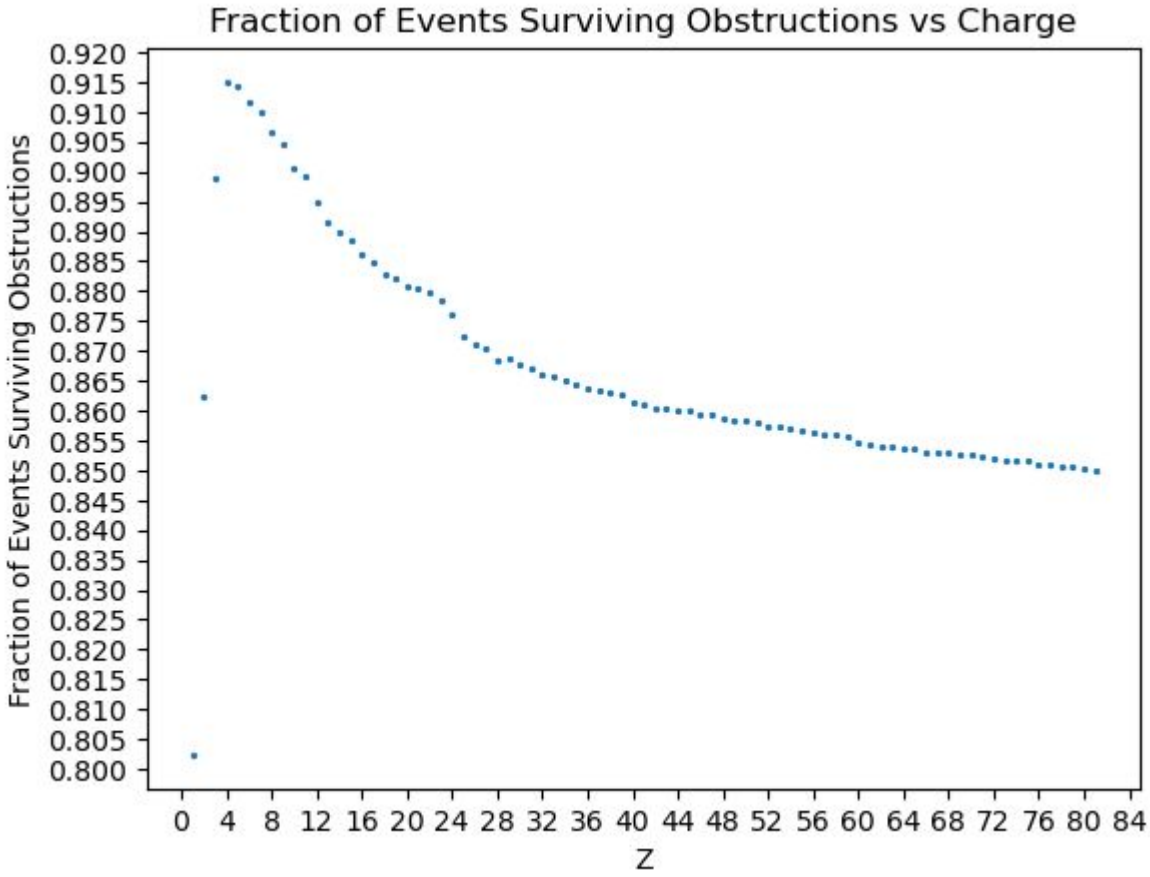
Fraction of Events Surviving Obstructions vs Charge
Fraction of Events Surviving Obstructions
0.920
0.915
0.910
0.905
0.900
0.895
0.890
0.885
0.880
0.875
0.870
0.865
0.860
0.855
0.850
0.845
0.840
0.835
0.830
0.825
0.820
0.815
0.810
0.805
0.800
0 4 8 12 16 20 24 28 32 36 40 44 48 52 56 60 64 68 72 76 80 84
Z

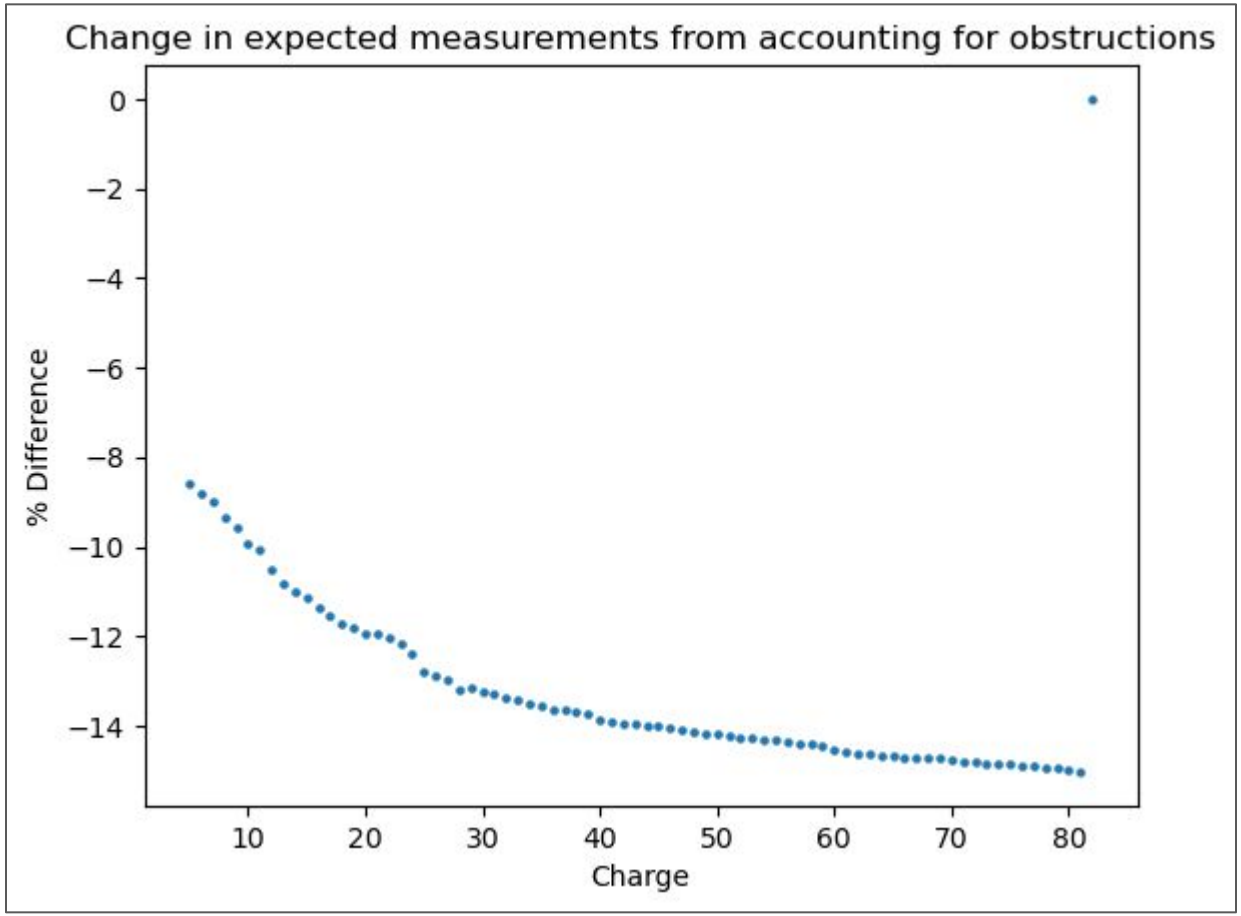
Change in expected measurements from accounting for obstructions
% Difference
0
−2
−4
−6
−8
−10
−12
−14
10
20
30
40
50
60
70
80
Charge

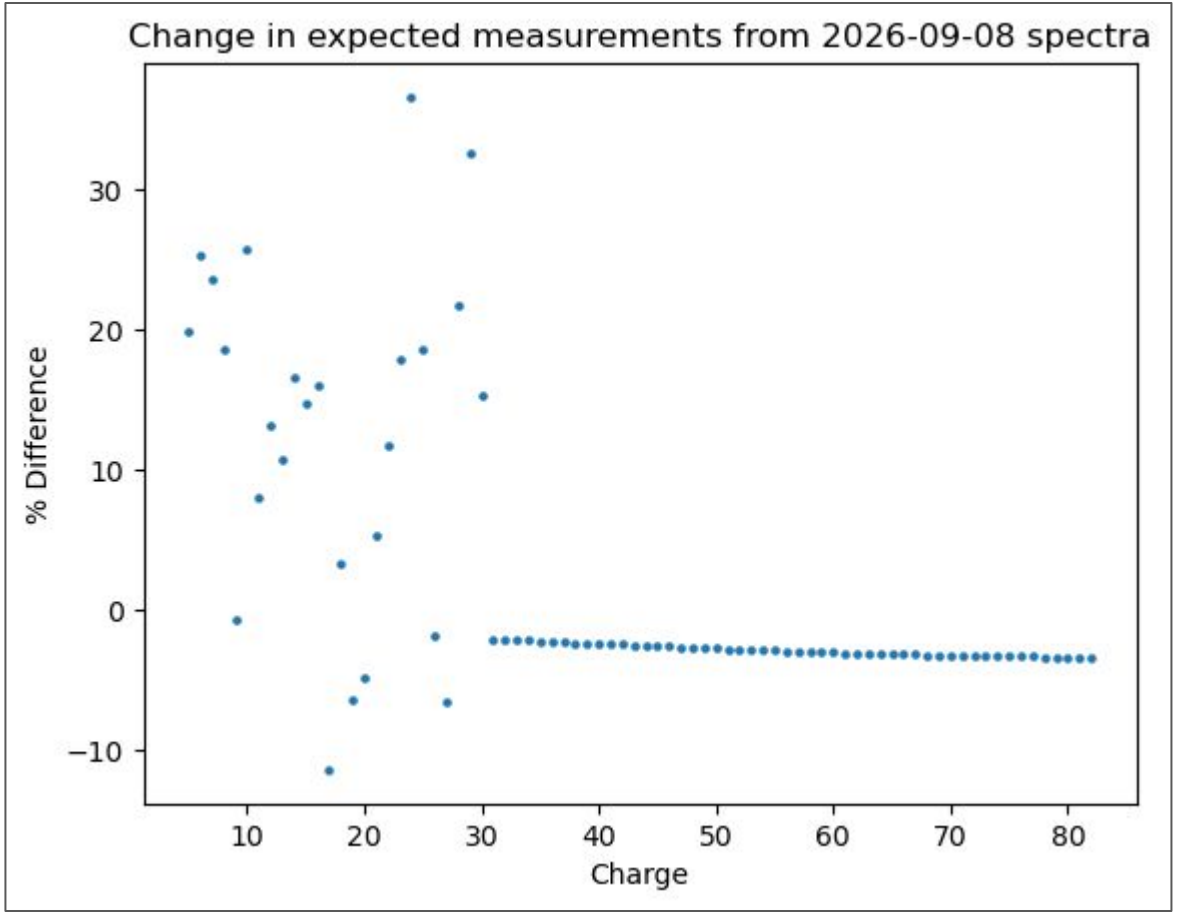
Change in expected measurements from 2026-09-08 spectra
% Difference
30
20
10
0
−10
10
20
30
40
50
60
70
80
Charge

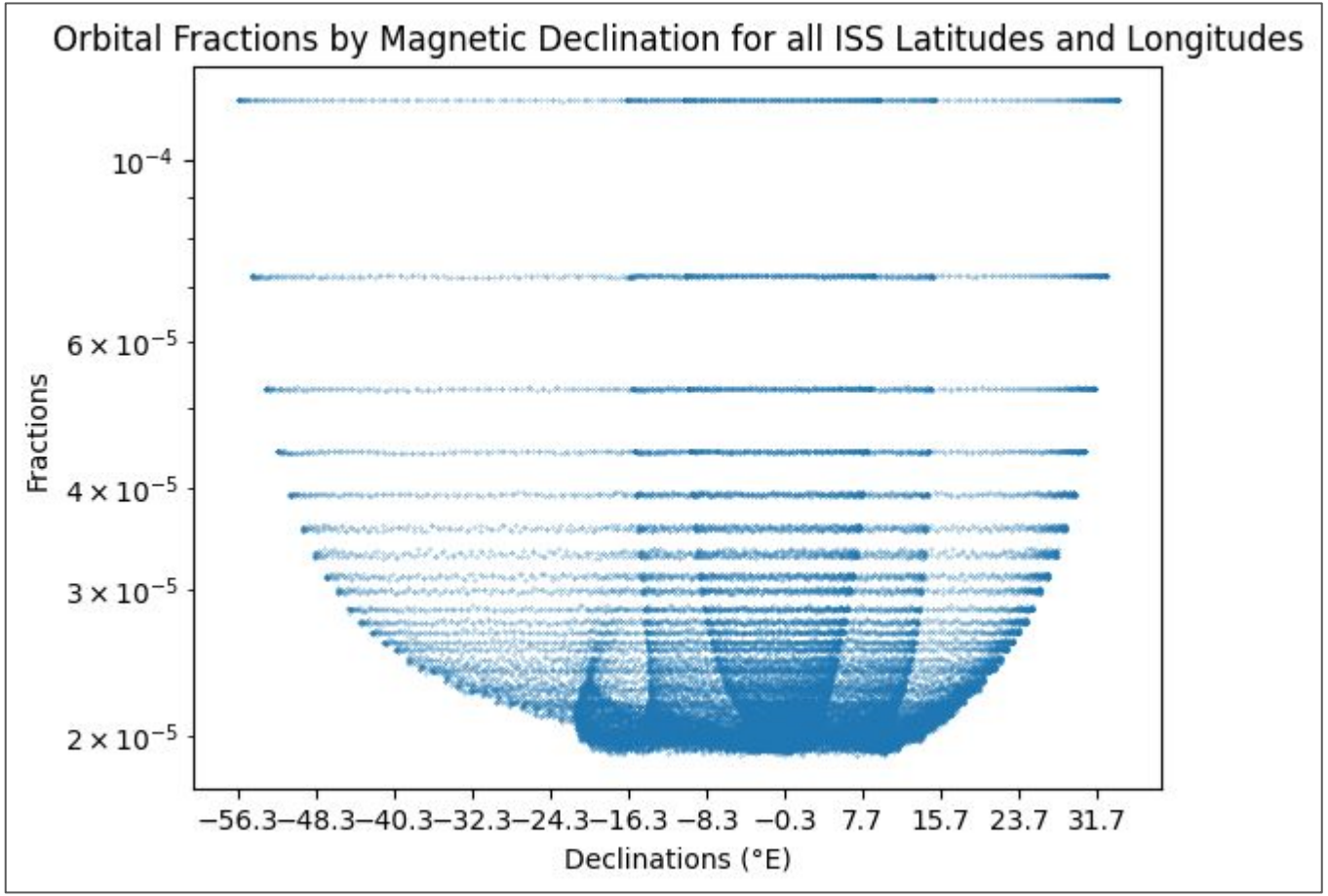
Orbital Fractions by Magnetic Declination for all ISS Latitudes and Longitudes
Fractions
10^{-4}
6×10^{-5}
4×10^{-5}
3×10^{-5}
2×10^{-5}
−56.3 −48.3 −40.3 −32.3 −24.3 −16.3 −8.3 −0.3 7.7 15.7 23.7 31.7
Declinations (°E)

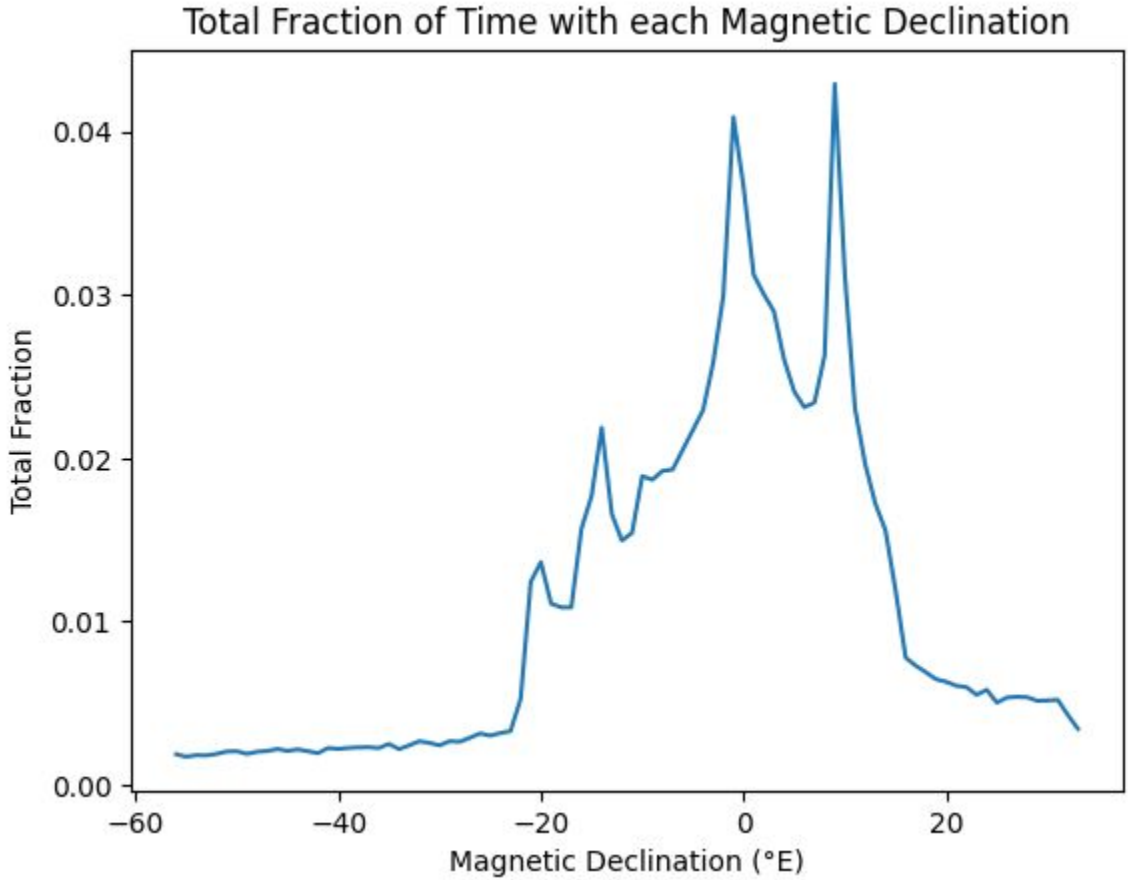
Total Fraction of Time with each Magnetic Declination
Total Fraction
0.00
0.01
0.02
0.03
0.04
−60
−40
−20
0
20
Magnetic Declination (°E)

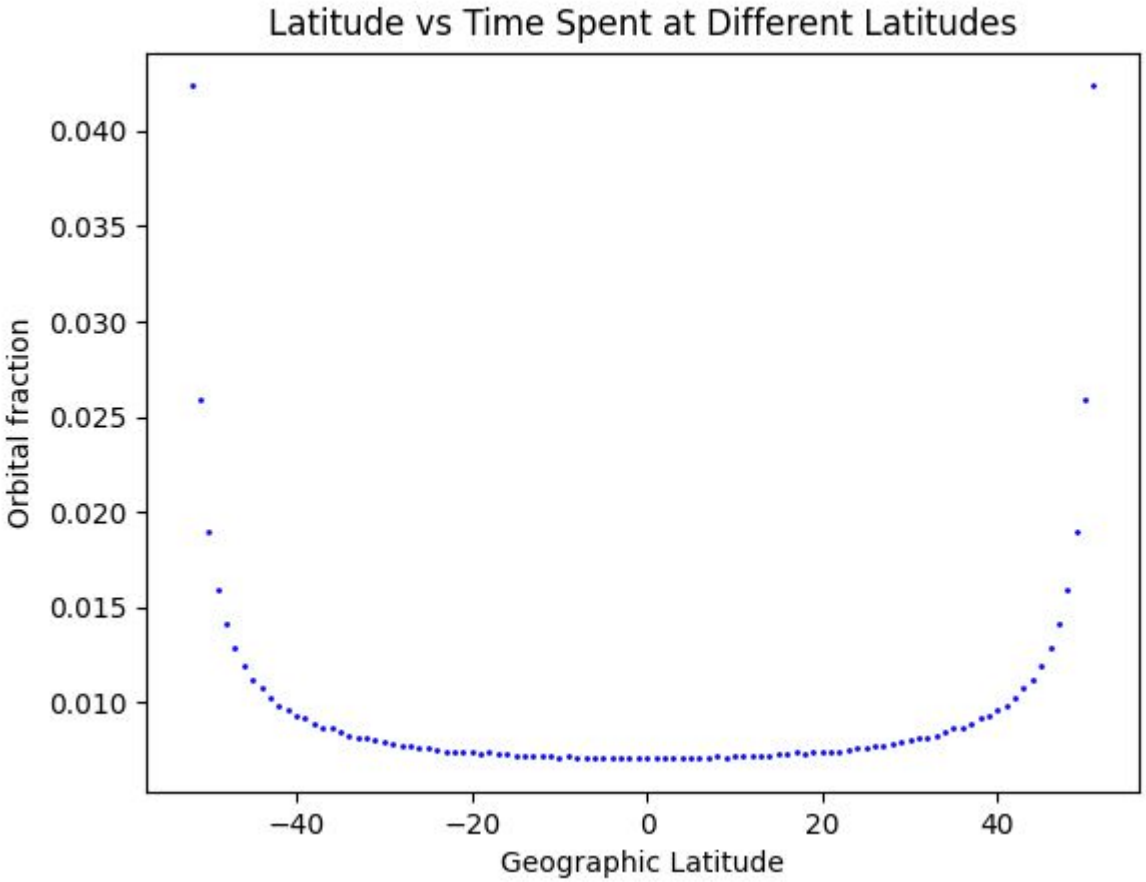
Latitude vs Time Spent at Different Latitudes
Orbital fraction
0.040
0.035
0.030
0.025
0.020
0.015
0.010
−40
−20
0
20
40
Geographic Latitude